Generating Bessel beams by use of localized modes

W. B. Williams and J. B. Pendry

Condensed Matter Theory Group, The Blackett Laboratory, Imperial College London, Prince Consort Road, London SW7 2BZ, UK

Received September 10, 2004; revised manuscript received November 26, 2004; accepted December 2, 2004

We propose a novel method for generating both propagating and evanescent Bessel beams. To generate propagating Bessel beams we propose using a pair of distributed Bragg reflectors (DBRs) with a resonant point source on one side of the system. Those modes that couple with the localized modes supported by the DBR system will be selectively transmitted. This is used to produce a single narrow band of transmission in κ space that, combined with the circular symmetry of the system, yields a propagating Bessel beam. We present numerical simulations showing that a propagating Bessel beam with central spot size of $\sim 0.5\lambda_0$ can be maintained for a distance in excess of $3000\lambda_0$. To generate evanescent Bessel beams we propose using transmission of a resonant point source through a thin film. A transmission resonance is produced as a result of the multiple scattering occurring between the interfaces. This narrow resonance combined with the circular symmetry of the system corresponds to an evanescent Bessel beam. Because propagating modes are also transmitted, although the evanescent transmission resonance is many orders of magnitude greater than the transmission for the propagating modes, within a certain distance the propagating modes swamp the exponentially decaying evanescent ones. Thus there is only a certain regime in which evanescent Bessel beams dominate. However, within this regime the central spot size of the beam can be made significantly smaller than the wavelength of light used. Thus evanescent Bessel beams may have technical application, in high-density recording for example. We present numerical simulations showing that with a simple glass thin film an evanescent Bessel beam with central spot size of $\sim 0.34\lambda_0$ can be maintained for a distance of $0.14\lambda_0$. By choice of different material parameters, the central spot size can be made smaller still.

OCIS codes: 260.1960, 260.5740, 240.0310, 230.1480.

1. INTRODUCTION

There exist solutions to Maxwell's equations that represent beams with well-defined narrow beam radii that do not undergo diffractive spreading. Such beams are known as Bessel beams. They can be propagating or evanescent.

Bessel beams were first proposed by Durnin and co-workers.[1,2] They pointed out that the Helmholtz equation is satisfied by a monochromatic wave propagating in the z direction with field amplitude $\Phi(x,y,z;\kappa) = \exp(ik_z z)J_0(k_r r)$, where $k_z^2 + k_r^2 = \kappa^2$, $x^2 + y^2 = r^2$, and J_0 is the zeroth-order Bessel function of the first kind. When $0 < k_r < \kappa$ this expression describes a propagating Bessel beam that does not undergo diffractive spreading and that has the same intensity distribution $J_0^2(k_r r)$ in every plane normal to the z axis. Of course the solution is rigorously exact only in free space. In any physical realization of a propagating Bessel beam, although diffractive spreading is initially repressed, after a fixed propagation distance the beam experiences a rapid drop-off in intensity.

An ideal propagating Bessel beam is described by the superposition of the set of plane waves with wave vectors lying on the surface of a cone[2] as shown in Fig. 1. There are a variety of methods for generating propagating Bessel beams,[1–6] all of which approximately produce such a superposition of plane waves, albeit limited by finite aperture effects. Durnin and co-workers, for example, illuminate a circular slit with collimated light.[1] Each point on the slit ideally acts as a point source that a lens then transforms into a plane wave. The superposition of each of these wave fields forms a propagating Bessel beam.

The half-width of the central peak of a Bessel beam is approximately k_r^{-1}. Therefore by making k_r larger, with $k_r < \kappa$, a narrower propagating Bessel beam can be produced. When $k_r > \kappa$ the beam width can be made smaller still, significantly smaller than the wavelength of light used. However, in this regime the beam ceases to be propagating and is evanescent. Evanescent Bessel beams have been investigated theoretically by Ruschin and Leizer.[7] With such beams we have a trade-off. On the one hand, the beam can be made very narrow. However, the field amplitude will decay exponentially. Evanescent Bessel beams may still have technical applications since, in contrast to a point source of radiation, in the ideal case the cross section of an evanescent Bessel beam does not deteriorate. Therefore the range is restricted only by the practical limit of the sensitivity of the detector used.

2. GENERATING PROPAGATING BESSEL BEAMS

To generate a propagating Bessel beam we consider a pair of distributed Bragg reflectors (DBRs) with a central cavity as shown in Fig. 2. The dielectric constants of the two layers in each Bragg reflector are ε_1 and ε_2, and each Bragg reflector has N bilayers. The unit cell of the Bragg stack is of thickness D and the first layer in the unit cell is of thickness d. The cavity is of length d_3 and has a dielectric constant ε_3.

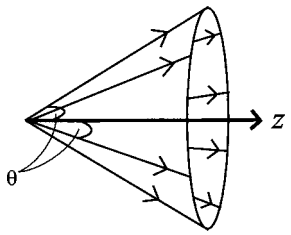

Fig. 1. Wave vectors lying on the surface of a cone.

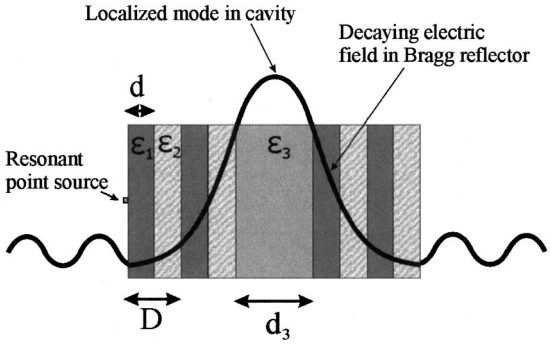

Fig. 2. Distributed Bragg reflectors with field decaying into Bragg stacks and localized mode in the cavity.

We investigate the transmission of a point source through the DBR structure. A small silver deposition could be used to act as a resonant point source scattering an incident beam to all wave vectors. Alternatively we could embed a laser diode inside the cavity. The DBR arrangement is then able to act as a filter that allows only modes corresponding to a narrow band of $k_r < \kappa$ to be transmitted. The symmetry of the system within the plane of stratification means that these modes are those with wave vectors lying on the surface of a cone. Therefore a propagating Bessel beam is generated.

Let us consider how this filtering of modes comes about. Working at a particular frequency, we select ε_1, ε_2, D, and d such that all the modes lie within a bandgap of each Bragg reflector. As illustrated in Fig. 2 the DBR arrangement can localize a mode within the cavity. Two conditions are necessary for this. First the mode must lie within the bandgap of the two Bragg reflectors so that the field corresponding to this mode is decaying within each of the Bragg reflectors. Second the cavity must be able to support a propagating mode. For this latter condition to be fulfilled at least half a wavelength must be able to "fit into" the cavity. Therefore d_3 must be greater than $\lambda_0/2\sqrt{\varepsilon_3}$.

Figure 3(a) shows the narrow band of localized modes when the cavity supports only one propagating mode. Only those incident wave vectors that are degenerate with these localized modes will be able to couple to them and thus have their transmission through the DBR system selectively enhanced. All other propagating modes will be suppressed by the bandgap. As the cavity length d_3 is increased beyond $\lambda_0/\sqrt{\varepsilon_3}$ other propagating modes can be supported within the cavity as shown in Fig. 3(b). Incident wave vectors degenerate with these modes will also be selectively transmitted across the DBR system. This results in a transmitted wave field that no longer corresponds to a Bessel beam. Therefore we must be sure to maintain the condition $\lambda_0/\sqrt{\varepsilon_3} > d_3 > \lambda_0/2\sqrt{\varepsilon_3}$.

We now have two scenarios. In the first we imagine that the cavity is of finite extent in the plane of the cavity. For example, it might consist of a cylindrical cavity. If we then tune to one of the modes of this cavity and ensure that the radiative losses through the ends are small, our source will fill the mode with energy, and the range of the Bessel beam will be predicted by the lateral extent of the mode $\sim L$, as shown in Fig. 4. Figure 5(a) shows the intensity of the mode with radial distance, here approximated by a simple top-hat function. The result is a Bessel beam that propagates unattenuated for a finite distance determined by the extent of the cavity and then collapses. This is the classic picture of a propagating Bessel beam.

In the second scenario the cavity can be regarded as being unbounded in the plane so that the energy is injected into a nonresonant state that decays exponentially from the injection point as a result of radiative losses into the Bessel beam. Now we must modify our argument for the intensity of the Bessel beam. Turning again to Fig. 4 we see that at a distance z from the cavity the beam draws its energy from a point on the cavity a radial distance $z \tan \theta$ from the injection point. Thus the intensity of the beam

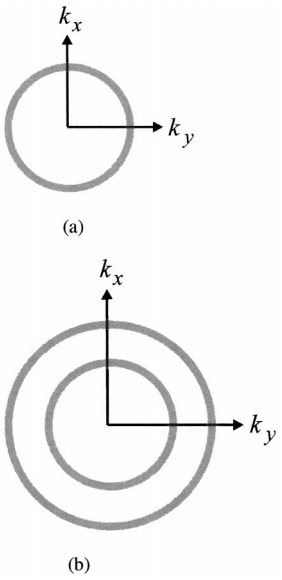

Fig. 3. (a) Narrow band of k_r corresponding to a localized mode. (b) Narrow bands of k_r corresponding to two localized modes.

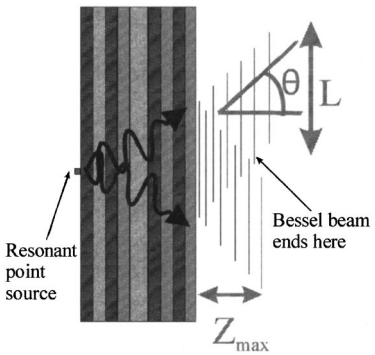

Fig. 4. Two-dimensional schematic of the wave field created with DBR arrangement.

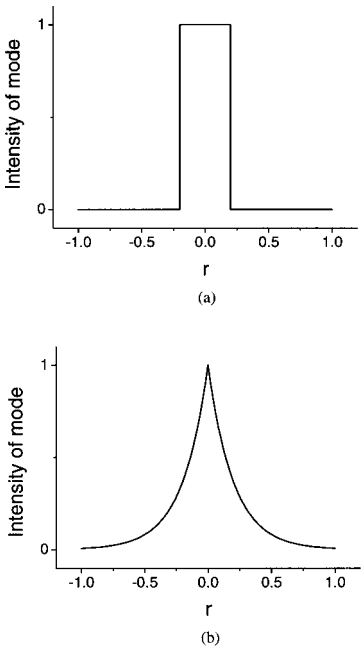

Fig. 5. (a) When the cavity is of finite size then the mode has a fixed lateral extent and its intensity as a function of r is approximated by a top-hat function. (b) When the cavity is unbounded the mode has an intensity that decays with radial distance.

along the z direction maps the radial distribution of energy, which in this case decays exponentially as shown in Fig. 5(b). So, paradoxically, even in the case where it is possible to have a propagating Bessel beam, it may in fact show exponential decay because of the profile from which it is generated. However, such a beam will maintain its radial profile for a greater distance than in the first scenario because of the presence of the tail of the mode's intensity.

The physical extent of the wave field L and the angle θ describing the direction of the cone of wave vectors completely define the resulting Bessel beam. The angle is dependent on the position of the transmission resonance in κ space. Furthermore, L is dependent on the width of the transmitted resonance Δk_r such that $L \approx 1/\Delta k_r$. Therefore the features of the resonance completely define the quality of the Bessel beam produced.

We investigate the proposed DBR system numerically using a transfer-matrix method[8] to calculate the band structure and transmission coefficients $T(k_r)$. Applying the Fourier–Bessel transform to our k-space transmission gives the real-space transmitted wave field $E_t = \int T_S(k_r)\exp[ik_z(z-z_2)]J_0(k_r r)k_r \mathrm{d}k_r$, where $T_S(k_r)$ is the transmission coefficient for s-polarized light and z_2 is the coordinate on the far side of the system.

We first present numerical results for a DBR arrangement with parameters as shown in Table 1, which could be experimentally realized to generate propagating Bessel beams at optical frequencies, corresponding to Bragg reflectors made from TiO_2 and SiO_2.[9] In our simulations we set the imaginary part of the dielectric constants in our DBR system to 0.0002 as suggested in Ref. 9. This corresponds to a Q factor of ~5000.

Figure 6 shows the band structure of a Bragg reflector with these parameters. For a fixed wavelength $\kappa = 2\pi/\lambda_0$ and by careful selection of D, d, ε_1, and ε_2 we ensure that all the modes with $k_r < \kappa$ lie within the first bandgap of each Bragg reflector. Thus all propagating modes except those that are degenerate with the localized mode within the DBR cavity are prevented from being transmitted.

Figure 7 shows the calculated transmitted intensity at z_2 on the far side of the DBR arrangement as a function of k_r. A narrow band of k_r centered around $0.83\,\kappa$ experiences enhanced transmission. Therefore we expect this to correspond to a propagating Bessel beam.

Figures 8(a) and 8(b) show the calculated real-space radial intensity profile and normalized real-space radial intensity profile plotted for various distances in the z direction. Sure enough, a Bessel-like radial intensity is present and a beam with central spot size of width $\sim 0.5\lambda_0$ can be maintained for a distance in excess of $3000\lambda_0$.

Figure 9 shows the transmitted intensity as a function of z plotted for fixed r. As explained, paradoxically, even though we have a propagating Bessel beam, the beam experiences exponential decay because of the profile from which it is generated.

Table 1. Parameters for a DBR Arrangement in Air

Parameter	Value for TiO_2/SiO_2 Bragg reflectors
$2\pi D/\lambda_0$	1.75
$2\pi d/\lambda_0$	1.038
$2\pi d_3/\lambda_0$	2.243
ε_1	$4.41+0.0002i$
ε_2	$2.074+0.0002i$
ε_3	$1.96+0.0002i$
N	12

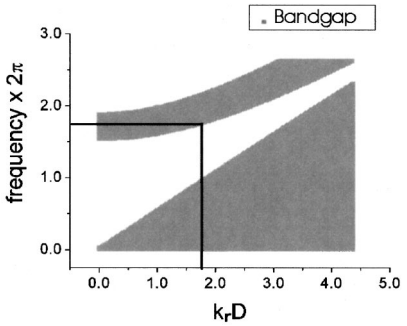

Fig. 6. Band structure of TiO_2/SiO_2 Bragg reflector. The horizontal line corresponds to the fixed frequency of light used. The vertical line corresponds to the cutoff between propagating and evanescent modes. All propagating modes lie within the bandgap.

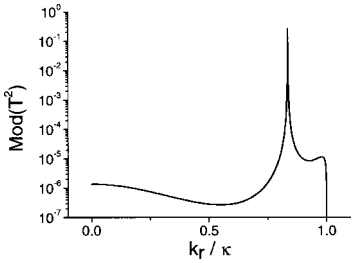

Fig. 7. Transmission as a function of k_r for a DBR arrangement with TiO_2/SiO_2 Bragg reflectors.

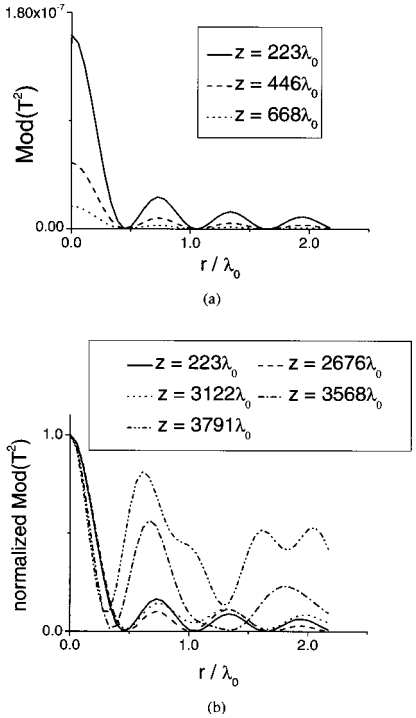

Fig. 8. (a) Transmitted intensity as a function of radial distance for a DBR with TiO_2/SiO_2 Bragg reflectors. (b) Normalized transmitted intensity as a function of radial distance for a DBR with TiO_2/SiO_2 Bragg reflectors.

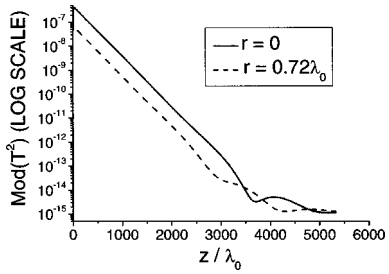

Fig. 9. Intensity plotted against z for fixed $r=0$ and $r=0.72\lambda_0$ showing paradoxical exponential decay of intensity for a propagating Bessel beam generated when the cavity is unbounded in the plane.

If we use the above approximation $L \approx 1/\Delta k_r$ we expect the maximum propagation distance to be $(L/2)/\tan\theta = 161\lambda_0$. This falls short of the actual value obtained and reflects the fact that $L \approx 1/\Delta k_r$ does not take account of the extended tails of the wave fields.

3. GENERATING EVANESCENT BESSEL BEAMS

To generate an evanescent Bessel beam we consider the simple arrangement shown in Fig. 10 consisting of a single film of thickness d_f and dielectric constant ε_f. We investigate the transmission of a point source through the film which, as with the DBR arrangement discussed in Section 2, could be a small silver deposition acting as a resonant point source to scatter an incident beam to all wave vectors.

The transmission through the film can be written in terms of a series for multiple scattering between the interfaces[10]:

$$T = t_{21}t_{32}\exp(ik_z d_f) + t_{21}r_{32}r_{12}t_{32}\exp(3ik_z d_f) + \cdots = \frac{t_{21}t_{32}\exp(ik_z d_f)}{1 - r_{32}r_{12}\exp(2ik_z d_f)}, \quad (1)$$

where t_{jk} and r_{jk} are the partial transmission and reflection Fresnel coefficients across the interfaces, and k_z is the magnitude of the component of the wave vector in the direction of propagation within the medium.

For imaginary k_z this function blows up when $r_{32}r_{12}\exp(2ik_z d_f)=1$. This resonance produces a narrow band of greatly enhanced transmission for modes with $k_r > \kappa$. If the intrinsic losses in the material are low, propagating modes with $k_r < \kappa$ have a transmission coefficient close to unity. The enhanced transmission for the resonant modes is many orders of magnitude greater than this.

Thus two competing wave fields are generated. One corresponds to the transmitted propagating modes where $T(k_r) \sim 1$ for $k_r < \kappa$. The second corresponds to the narrow band of selectively enhanced evanescent modes where $k_r > \kappa$. Because of the circular symmetry of the system, in a manner analogous to that described in Section 2 this second evanescent wave field describes an evanescent Bessel beam.

Although the evanescent beam wave field is initially many orders of magnitude greater than the propagating wave field, it is of course decaying exponentially. Thus within a short distance in the z direction the propagating modes swamp the evanescent ones. However, for sufficiently small z the evanescent Bessel beam dominates, and within this regime the resulting transmitted intensity has a Bessel-like radial profile with a subwavelength central peak as defined by the position of the resonance. This is the interesting regime in which our technique may find applications fulfilling particular technological needs. By increasing the dielectric constant of the film and re-

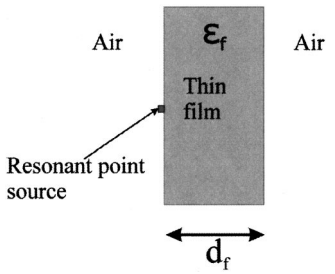

Fig. 10. Transmission through a thin dielectric film to generate an evanescent Bessel beam.

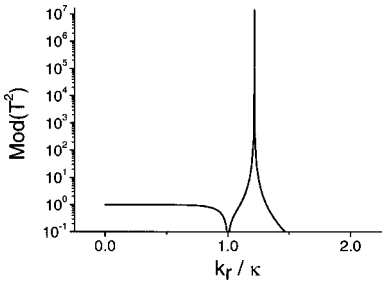

Fig. 11. Transmission as a function of k_r for a thin film with $\varepsilon_f = 1.96 + 0.0001i$ and $d_f = 0.357\lambda_0$.

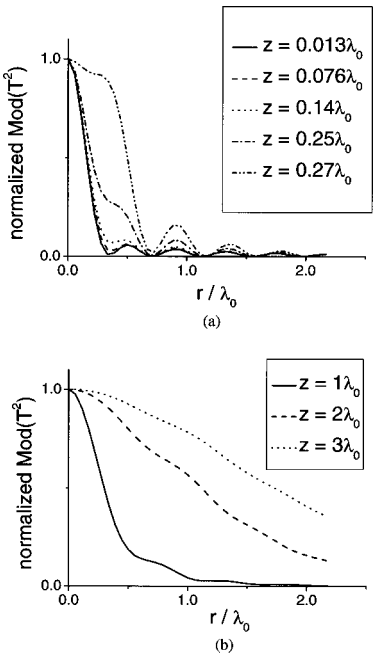

Fig. 12. (a) Normalized transmitted intensity as a function of radial distance for thin film with $\varepsilon_f = 1.96 + 0.0001i$ and $d_f = 0.357\lambda_0$ for fixed z values up to $z = 0.27\lambda_0$. (b) Normalized transmitted intensity as a function of radial distance for thin film with $\varepsilon_f = 1.96 + 0.0001i$ and $d_f = 0.357\lambda_0$ for fixed z values up to $z = 3\lambda_0$.

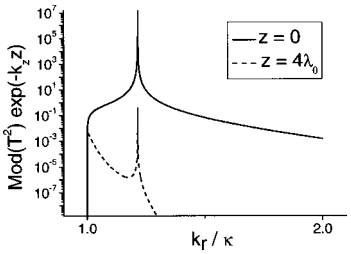

Fig. 13. $|T^2|\exp(-k_z z)$ for a thin film with $\varepsilon_f = 1.96 + 0.0001i$ and $d_f = 0.357\lambda_0$.

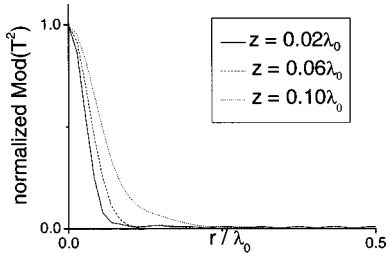

Fig. 14. Normalized transmitted intensity as a function of radial distance for thin film with $\varepsilon_f = 100.0 + 0.0001i$ and $d_f = 0.05\lambda_0$ for fixed z values up to $z = 0.10\lambda_0$.

ducing its thickness one can force the position of the resonance in k_r to move to higher values. Hence one has control over the subwavelength beam radius within this regime.

Once the propagating modes start to dominate, the resulting wave field becomes that corresponding to a point source. This is because, for low losses, the thin film has no effect on propagating modes, which are all transmitted.

We present numerical results for a thin glass film with $d_f = 0.357\lambda_0$ and $\varepsilon_f = 1.96 + 0.0001i$. Figure 11 shows the transmitted intensity at z_2' on the far side of the thin film as a function of k_r. For the propagating modes corresponding to $k_r < \kappa$ the transmission $T(k_r) \approx 1$. A narrow band of k_r centered around 1.21 κ experiences enhanced transmission, and this narrow band corresponds to an evanescent Bessel beam.

Figures 12(a) and 12(b) show the calculated normalized real-space intensity profile plotted for various distances in the z direction. For sufficiently small z the resulting profile is indeed Bessel-like, with a central spot size of $\sim 0.34\lambda_0$ that is maintained for a distance of $0.14\lambda_0$.

However, within a couple of wavelengths in the z direction the profile is no longer dominated by a central peak. Figure 13 shows $|T^2|\exp(-k_z z)$ as a function of k_r for evanescent modes. Within four wavelengths, the magnitude of the resonance is reduced to ≈ 0.5 by the exponential, and this explains why it no longer dominates.

If a yet smaller initial spot size is desired, this can be achieved by selecting a film of higher dielectric constant and with reduced thickness. Figure 14, for example, shows the calculated normalized real-space intensity profile plotted for various distances in the z direction for a film with $d_f = 0.05\lambda_0$ and $\varepsilon_f = 100.0 + 0.0001i$. For sufficiently small z the resulting profile has a central spot size of $\sim 0.08\lambda_0$ that is maintained for a distance of $0.06\lambda_0$.

To extend the range over which the evanescent resonance dominates, we need to suppress the transmission of propagating modes. To do this one might consider the use of a multilayer structure to produce a bandgap. However, any such multilayer structure will result in more than a single evanescent resonance. Multiple resonances yield wave fields that do not correspond to Bessel beams.

4. CONCLUSION

The technique we suggest is able to produce both propagating and evanescent Bessel beams. Our calculations show that by using a DRB with the parameters we propose, a propagating Bessel beam with a central spot size of $\sim 0.5\lambda_0$ can—remarkably—be maintained for a distance in excess of $3000\lambda_0$. Our calculations also show that by use of only a simple thin-film arrangement, evanescent Bessel beams can be generated that have a central spot size of $\sim 0.34\lambda_0$ that is maintained for a distance of $0.14\lambda_0$ (although, of course, the field is decaying exponentially with z). For both of these systems, by appropriate choice of optical parameters and geometry the central spot size of the Bessel beam produced can be controlled. However, since the central spot size is approximately k_r^{-1} there is a limit on how narrow a propagating Bessel beam can be when $k_r < \kappa$. In the case of the evanescent Bessel beam, this limitation is overcome with the trade-off that the field decays exponentially.

Let us compare our simulated results with other techniques for generating propagating Bessel beams. For relatively large spot size (compared with the wavelength) Durnin *et al.*[1] have produced propagating beams with spot sizes of ≈ 0.2 mm ($316\lambda_0$) that are maintained for almost 1 m ($1.6 \times 10^6 \lambda_0$) with use of 633-nm-wavelength light. Our technique is suitable for generating much smaller beam sizes than this albeit of shorter range. More directly comparable with our technique, using an axicon

Garcés-Chávez *et al.*[11] have generated Bessel beams with central spot sizes of ~500 nm ($0.47\lambda_0$) that are maintained for approximately 4 mm ($3760\lambda_0$) with use of 1064-nm light. These parameters are very similar to those we are able to obtain from our simulations in the propagating cases.

By reducing the losses in our proposed DBR system and thus making the resonance in κ space yet narrower, the propagation distance of the Bessel beam can be increased. Whether such an extension is favorable over other methods of beam generation will depend on the details of the particular application one has in mind.

It is worth commenting on the flexibility of the method of beam generation we propose. Since Maxwell's laws are scalable, by scaling the geometry of the DBR arrangement or thin film one is able to extend the technique into a variety of frequency regimes. It is an engineering problem rather than a problem of principle, involving meeting the challenge to find materials with appropriate dielectric constants at the wavelengths being used.

Bessel beams have a variety of potential applications. In the microwave region propagating Bessel beams may have uses in radar technology and, at radio frequencies, in covert communications. The most important uses are likely to be in the optical regime, where these beams could play a role in the development of optical tweezers[11,12] and in high-density recording. It is in this latter role that evanescent Bessel beams and the subwavelength beam diameters that such beams exhibit could prove useful tools in certain technologies.

ACKNOWLEDGMENTS

Wayne Williams is supported by the European Community Information Society Technologies program Development and Analysis of Left-Handed Materials, project IST-2001-35511. J. B. Pendry is supported by the Engineering and Physical Sciences Research Council, the European Union under project FP6-NMP4-CT-2003-505699, and U.S DoD Office of Naval Research MURI grant N00014-01-1-0803.

The e-mail address of corresponding author Wayne Williams is wayne.williams@imperial.ac.uk.

REFERENCES

1. J. Durnin, J. J. Miceli, Jr., and J. H. Eberly, "Diffraction-free beams," Phys. Rev. Lett. **58**, 1499–1501 (1987).
2. J. Durnin, "Exact solutions for nondiffracting beams. I. The scalar theory," J. Opt. Soc. Am. A **4**, 651–654 (1987).
3. J. Durnin and J. H. Eberly, "Diffraction-free arrangement," U.S. patent 4,852,973 (1 August 1989).
4. J. Eberly, Department of Physics and Astronomy, University of Rochester, Rochester, New York 14627 (personal communication, 2004).
5. A. Vasara, J. Turunen, and A. T. Friberg, "Realization of general nondiffracting beams with computer-generated holograms," J. Opt. Soc. Am. A **6**, 1748–1754 (1989).
6. R. M. Herman and T. A. Wiggins, "Production and uses of diffractionless beams," J. Opt. Soc. Am. A **8**, 932–942 (1991).
7. S. Ruschin and A. Leizer, "Evanescent Bessel beams," J. Opt. Soc. Am. A **15**, 1139–1143 (1998).
8. M. Born and E. Wolf, *Principles of Optics* (Pergamon, Oxford, UK, 1975).
9. W. M. Robertson, "Experimental measurement of the effect of termination on surface electromagnetic waves in one-dimensional photonic bandgap arrays," J. Lightwave Technol. **17**, 2013–2017 (1999).
10. J. B. Pendry, *Low Energy Electron Diffraction* (Academic, London, 1974).
11. V. Garcés-Chávez, D. McGloin, H. Melville, W. Sibbett, and K. Dholakia, "Simultaneous micromanipulation in multiple planes using a self-reconstructing light beam," Nature (London) **419**, 145–147 (2002).
12. D. McGloin, V. Garcés-Chávez, and K. Dholakia, "Interfering Bessel beams for optical micromanipulation," Opt. Lett. **28**, 657–659 (2003).